

Ionic conductivity in poly(propylene glycol) complexed with lithium and sodium triflate

I. Albinsson, B.E. Mellander, and J. R. Stevens

Citation: [The Journal of Chemical Physics](#) **96**, 681 (1992); doi: 10.1063/1.462453

View online: <http://dx.doi.org/10.1063/1.462453>

View Table of Contents: <http://scitation.aip.org/content/aip/journal/jcp/96/1?ver=pdfcov>

Published by the [AIP Publishing](#)

Articles you may be interested in

[Resolving distribution of relaxation times in poly\(propylene glycol\) on the crossover region](#)

J. Appl. Phys. **95**, 3131 (2004); 10.1063/1.1650888

[Effects of dynamic spatial disorder on ionic transport properties in polymer electrolytes based on poly\(propylene glycol\)\(4000\)](#)

J. Chem. Phys. **107**, 9168 (1997); 10.1063/1.475208

[Dielectric and conductivity relaxation in poly\(propylene glycol\)–lithium triflate complexes](#)

J. Chem. Phys. **94**, 6323 (1991); 10.1063/1.460420

[Effect of high pressure on electrical relaxation in poly\(propylene oxide\) and electrical conductivity in poly\(propylene oxide\) complexed with lithium salts](#)

J. Appl. Phys. **60**, 2665 (1986); 10.1063/1.337093

[Ionic conductivity and mobility in network polymers from poly\(propylene oxide\) containing lithium perchlorate](#)

J. Appl. Phys. **57**, 123 (1985); 10.1063/1.335386



Ionic conductivity in poly(propylene glycol) complexed with lithium and sodium triflate

I. Albinsson and B.-E. Mellander

Department of Physics, Chalmers University of Technology, S-412 96, Göteborg, Sweden

J. R. Stevens

Guelph-Waterloo Program for Graduate Work in Physics, Guelph Campus, Department of Physics, University of Guelph, Guelph, Ontario N1G 2W1, Canada

(Received 17 July 1991; accepted 18 September 1991)

Conductivity and viscosity measurements have been made for poly(propylene glycol)-MCF₃SO₃ (M = Li, Na) complexes in order to examine more closely the Vogel–Tammann–Fulcher (VTF) empirical relationship which has been found in previous reports to provide a good fit to the experimental data. Further, a dynamic bond percolation model of ion conduction in polymer electrolytes has predicted VTF behavior and an inverse relationship between molar conductivity and viscosity or Walden “rule” behavior. We find that deviations occur from both the VTF and Walden empirical relationships and propose a modest alteration in the form of the dynamic percolation model for ions moving in polyether systems.

I. INTRODUCTION

There is a broad current interest in solid polymeric electrolytes for such applications as electrochromic devices, batteries, and fuel cells. One of the simpler polymer-salt materials is obtained by using polyethers such as poly(propylene glycol) (PPG) with salts such as alkali and alkali metal perchlorates and triflates. There have been extensive studies of the ionic conductivity in these systems. It has been generally found^{1,2} that the ionic d.c. conductivity σ varies with temperature according to the empirical–phenomenological Vogel–Tammann–Fulcher (VTF) relationship, viz.

$$\sigma = A_{\sigma} T^{-1/2} \exp[-E_{\sigma}/k_B(T - T_0)], \quad (1)$$

where E_{σ} is a pseudoactivation energy, k_B is the Boltzmann constant, A_{σ} is a constant proportional to the number of carrier ions, and T_0 is a reference temperature usually associated with the ideal glass transition temperature at which “free” volume disappears, or the temperature at which the configurational entropy becomes zero. In either case, T_0 usually lies 35–50 K below T_g . The nature of the prefactor in Eq. (1) is discussed from several points of view by Ratner *et al.*³ and Papke, Ratner, and Shriver.⁴ These discussions present arguments which range from those based on the empirical Doolittle equation⁵ for shear viscosity η , where

$$\eta = B \exp[\text{constant}(v_0/v_f)], \quad (2)$$

or relationships adjusted to it, to those based on phenomenological configurational entropy models.⁴ Inherent at some point in these developments is the concept of “average free volume per molecule” v_f and the van der Waals’ volume v_0 . Also implicit is the Nernst–Einstein relationship for interacting charge carriers⁶

$$\sigma = q^2 \langle \Delta n^2 \rangle DV/k_B T \quad (3)$$

and an inverse relationship between the self-diffusion constant D and η as found in the Stokes–Einstein relation

$$D = k_B T/(6\pi R\eta), \quad (4)$$

where R is the ion radius. Gefen and Goldhirsch⁷ find that

Eq. (3), in which $\langle \Delta n^2 \rangle$ is the average fluctuation of carrier density, V is the volume, and q the carrier charge, holds for disordered random media. In the development of Eq. (3), mobility ($\mu = Dq/k_B T$) is defined as velocity per unit electric field, whereas in the original Einstein relation, mobility ($\mu = D/k_B T$) was defined as velocity per unit force.⁸ The form of Eq. (3) usually quoted³ contains n , the charge particle density, in place of $\langle \Delta n^2 \rangle$. In the straightforward “Einstein-type” derivation (concentrating only on the charged particles in the mixture and assuming motion only in the z direction), the equilibrium condition $-Dq(\partial n/\partial z) + \sigma E = 0$ together with the pressure gradient equation $\partial P/\partial z = nqE$ are combined to produce the Nernst–Einstein result $(1/n)(\partial P/\partial n) = q^2 D/\sigma$. For noninteracting particles, $\partial P/\partial n$ is obtained from the ideal gas law ($\partial P/\partial n = k_B T$), but for interacting particles $\partial P/\partial n = nk_B T/V \langle \Delta n^2 \rangle$, a purely thermodynamic result obtained via the compressibility. (A rigorous result would take into consideration the fact that the liquid electrolyte is a solution of charged particles.)

The temperature dependence for σ in Eq. (3) comes in through D assuming negligible contribution from $\langle \Delta n^2 \rangle/k_B T$ and therefore through η and $v_f = \beta \bar{v}_M(T - T_0)$ in Eq. (2), where Maxwell–Boltzmann statistics govern particle motions [$\beta \propto T^{-1/2}$ in Eq. (2)]. β is the expansion coefficient and \bar{v}_M is the mean molecular volume over the range (T, T_0) . Equations (1) and (3) are developed on the premise that the forces acting to produce diffusional motion are small and that the moving particles do not require an activation energy to move from one site to the next; the “molecular cage” just opens up and a particle moves through.⁸

The inverse relationship between conductivity and viscosity implicit in Eqs. (3)–(4) has long been recognized. Walden⁹ proposed that the product of the molar conductivity at infinite dilution Λ_{∞} and the shear viscosity η of the pure solvent is constant, independent of temperature in a given solvent and independent of solvent at a given tempera-

ture. The usefulness of Walden's "rule" has been limited by the solvation characteristics of various solvents for the same salt; different solvents solvate the same ions to different extents, which in turn effects the viscosity.

It has also been recognized for some time that the motion of ions in an ion conducting material is coupled to the motion of structural elements in the material. In an ionic crystal, there exists different kinds of movable lattice defects and in a polymeric liquid segmental motion of the polymer chains. Recently, Druger, Nitzan, and Ratner¹⁰ and co-workers have used dynamic percolation theory to describe the diffusion of small particles, such as ions, in a polymeric medium which is randomly disordered and where the entire medium is undergoing structural relaxation on a time scale shorter than the experimental time scale; spatial correlations are disregarded. The development of this theory, summarized by Ratner and Nitzan,³ has been extended by Granek and Nitzan¹¹ to include spatial correlations in the context of a many-bond effective medium approximation using the formalism of Harrison and Zwanzig.¹² For a single time scale for segmental (or lattice) rearrangement or relaxation and for a Poisson distribution of renewal times with ensemble average τ_R , the frequency-dependent diffusion coefficient in dynamically disordered systems (i.e., above T_g) is predicted to be

$$D(\omega, \lambda) = D_0(\omega - i\lambda), \quad (5)$$

where $\lambda = 1/\tau_R$ and $D_0(\omega)$ is the frequency-dependent diffusion coefficient in a medium with static disorder (i.e., below T_g). For more than one time scale for segmental rearrangement, this relation is no longer valid.¹¹

Ratner and Nitzan³ claim that with certain reasonable assumptions relating viscosity to segmental relaxation, there is an inverse relationship between D and η and that a VTF temperature dependence exists. This infers a Walden type relationship, given the validity of Eq. (3) in disordered random media.⁷ They propose a Walden type product [given Eq. (3)].

$$D\eta = mc_s^2 \langle r^2 \rangle_{0,R} p / a^2, \quad (6)$$

where m is the mass of the diffusing particle, c_s is the speed of sound in an elastomer, $\langle r^2 \rangle_{0,R}$ is the mean-squared "displacement" in the medium with static disorder during one renewal interval of the corresponding dynamically disordered system averaged over the renewal time distribution, p is the probability that a "bond" or pathway is available for ionic motion between sites,^{10,11} or the probability that a site will be available,^{3,13} and a is the mean distance between sites. In other words, all sites may be occupied by a charge carrier and p is the fraction of nearest-neighbor paths that are allowed for a site independent of whether or not the carrier is on the site. For those "bonds" or sites which have an "available" or "open" probability p , the probability for a charge carrier to hop is w ; otherwise the hopping probability is zero.

There is considerable evidence in the literature¹⁴⁻¹⁶ that the coupling of ions with polymer segmental motion is important for good conductivity up to about 100 Poise¹⁴ and that there is a VTF temperature dependence as in Eq. (1).

For the special case of d.c. diffusion ($\omega = 0$), Eq. (5) yields^{10,11}

$$D(0, \lambda) = \langle r^2 \rangle_{0,R} / 2d\tau_R. \quad (7)$$

The system is assumed to be isotropic with Euclidean dimensionality d . r is essentially the radius of gyration of a walk performed by a diffuser on the "unstirred" or static system.^{3,13}

If a diffuser can completely explore a finite connected percolation cluster of any size prior to its rearrangement or renewal, $\langle r^2 \rangle_{0,R}$ scales¹³ as $(p_c - p)^{-(2\nu - \beta)}$. When $p \rightarrow p_c$, the correlation-length exponent ξ diverges as $(p_c - p)^{-\nu}$. The probability to be in the infinite cluster $P_\infty(p)$ is zero below p_c and is proportional to $(p - p_c)^\beta$ for $p > p_c$.¹⁷ One can think of a fluctuating polymer segment which can open or block ionic pathways with a characteristic switching rate of λ . Approaching the critical value p_c from below, the diffusion diverges due to the divergence of $\langle r^2 \rangle_{0,\pi}$. Thus,

$$D(0, \lambda) \propto (p_c - p)^{-(2\nu - \beta)} / \tau_R. \quad (8)$$

For $d = 3$, $2\nu - \beta \approx 1.3$ and τ_R can be identified with the local viscosity in a polyether-salt electrolyte.

In such an electrolyte, the cation sites are defined by the ether oxygens to which the cation is coordinated; from crown-ether chemistry, there are approximately four ether oxygens for Li^+ and 5 for Na^+ . For anions, the sites are voids within the polymer segments; the anion is usually not solvated unless the polyether chains are hydroxyl terminated and then only a fraction are affected.

A percolation threshold below which diffusion is not observed does not exist in dynamic or "stirred" percolation models; a diffuser can travel arbitrarily far from its origin for all concentrations. However, for the case discussed above (long observation time and large values of τ_R compared to the rate at which the diffuser travels), a remnant of threshold behavior is observed since D changes substantially in this region. The percolation threshold is "smeared" rather than being absent. An exact calculation in one dimension is given for this case.^{3,10}

If τ_R is less than the time it takes for a diffuser to explore a finite, connected region, then $D(0, \lambda) = pD_0(0)$. Other limits are explored by various authors^{3,11,13} and references therein.

As a basis for another approach to using percolation ideas to explain ion conductivity in polymer electrolytes, we refer to the work of Ast¹⁸ who discusses the case of static bond percolation in which there are two phases with conductivities σ_1 and σ_2 . Using the many-bond effective medium approximation as did Harrison and Zwanzig (following Kirkpatrick¹⁹), they find (with Landauer²⁰) the following expression for the conductivity of the medium:

$$4\sigma = k_2 - k_1 x + [(k_2 - k_1 x)^2 + 8\sigma_1 \sigma_2]^{1/2}. \quad (9)$$

$k_1 = 3(\sigma_1 - \sigma_2)$, $k_2 = 2\sigma_1 - \sigma_2$, and x is the volume fraction of phase 2. The result is based on the assumption that all of the randomly distributed clusters of phases 1 and 2 are spherically symmetric and that there is no spatial correlation between them. For a polymer electrolyte, one can visualize one region as containing a collection or cluster of "free" solvent separated ions and solvent separated charged aggregates of ions (phase 1) and a second region (phase 2) where neutral species dominate. In polymer electrolytes, these two

regions are stirred continually by the fluctuating chain segments within which they are embedded; the two phases, including the clusters, are being reformed or renewed continually on an average time scale of the same order as the average structural relaxation time. If one assumes that this time is proportional to the local or microscopic viscosity, one can argue phenomenologically that dividing Eq. (9) by the dimensionless η/η_0 (related to τ_R) would give a conductivity for the stirred medium. η_0 is the viscosity of the pure polymer. Here we would assume that, for the low molecular weights 10 000 or less, there is a simple proportionality between the local shear viscosity and the bulk shear viscosity.

Bunde, Dieterich, and Roman^{21,22} consider a lattice model of a fraction p of insulating phase in a conducting matrix; the case of Al_2O_3 in ionic conductors such as LiI , for example. This model places special emphasis on the role of an enhanced interface conductivity predicting a critical concentration p'_c related to the interface "bonds" only. The results of Bunde, Dieterich, and Roman^{21,22} suggest that the limiting value of the self-diffusion coefficient $D(p, \infty)$ should follow Eq. (10)

$$D(p, \infty) \sim (p'_c - p)^{-5}. \quad (10)$$

Equation (10) describes the characteristic behavior of random superconducting networks where $s \simeq 0.75$ for three dimensions.²³ Considering the form of Eq. (8) for stirred systems, Eq. (10) divided by τ_R could be a possible model for polymer electrolytes in which we consider a description similar to that discussed above.

The objective of this research is to examine closely the VTF and Walden relationships for PPG complexed with LiCF_3SO_3 and NaCF_3SO_3 and for which d.c. conductivity and viscosity are measured. We show where deviations occur from these relationships, probably due to ion association (as anticipated by Ratner and Nitzan³). Attempts will be

made to use percolation concepts to understand our conductivity results.

II. EXPERIMENT

LiCF_3SO_3 and NaCF_3SO_3 (Aldrich Chemical Company Inc.) stated to be 97% pure, and monodisperse poly(propylene glycol) of molecular weights 425 and 4000 (Polysciences) were used. The salt was dried in a vacuum oven first at 125 °C for 24 h and then at 20 °C for 24 h more before being used. The polymer was filtered and then dried in a vacuum oven at room temperature for 24 h and then, under a vacuum of 10^{-3} Pa, stringently freeze dried using freeze-pump-thaw cycles. While still under vacuum, the polymer was transferred to an argon atmosphere and heated to 77 °C where the salt was dissolved directly into the heated polymer using a magnetic stirrer. Concentrations varied from an ether oxygen to alkali metal (O:M) ratio of about 90 000:1 to 11:1 for LiCF_3SO_3 in PPG 4000. (For the convenience of the reader, Table I lists various concentration units for the PPG 4000- LiCF_3SO_3 complex. For our analysis, we use concentrations in mole(salt) per kilogram of salt plus solvent.) For PPG 425- LiCF_3SO_3 concentrations ranged from O:M = 200:1 to O:M = 12.5:1 and for PPG 4000- NaCF_3SO_3 from O:M = 1000:1 to O:M = 8.1. The doped samples were stored in a dry atmosphere before being transferred, in an argon atmosphere, to the sample holders for the conductivity and differential scanning calorimetry (DSC) measurements.

The complex impedance was measured using a computer controlled HP4274A LCR meter over a frequency range of 100 Hz–100 kHz with an applied signal of 20 mV. The sample was measured between cylindrical stainless steel electrodes, 10.3 mm in diameter, and varied in thickness from 0.9 to 1.3 mm. The sample temperature was measured

TABLE I. Conversion table for PPG 4000 + LiCF_3SO_3 at 22 °C.

Mol %	O:M	c (mol/kg)	$c^{1/2}$ (mol/kg) ^{1/2}	c (mol/l)	$c^{1/2}$ (mol/l) ^{1/2}
0	∞	0	0	0	0
0.001 11	90 100	0.000 192	0.0139	0.000 193	0.0139
0.003 44	29 100	0.000 592	0.0243	0.000 596	0.0244
0.014	7 140	0.002 34	0.0484	0.002 36	0.0485
0.037	2 700	0.006 44	0.0802	0.006 49	0.0805
0.107	934	0.018 4	0.136	0.018 6	0.136
0.331	301	0.056 7	0.238	0.057 4	0.240
0.498	200	0.085 1	0.292	0.086 4	0.294
0.751	132	0.128	0.358	0.130	0.361
0.989	100	0.168	0.410	0.172	0.415
1.49	66.1	0.250	0.500	0.259	0.508
1.96	50	0.327	0.572	0.340	0.583
2.45	39.8	0.405	0.636	0.424	0.651
3.23	30	0.527	0.726	0.558	0.747
4.16	23.0	0.669	0.818	0.718	0.847
5.88	16	0.923	0.960	1.014	1.007
6.16	15.2	0.960	0.980	1.059	1.029
7.69	12	1.174	1.083	1.320	1.149
8.07	11.4	1.223	1.106	1.381	1.175

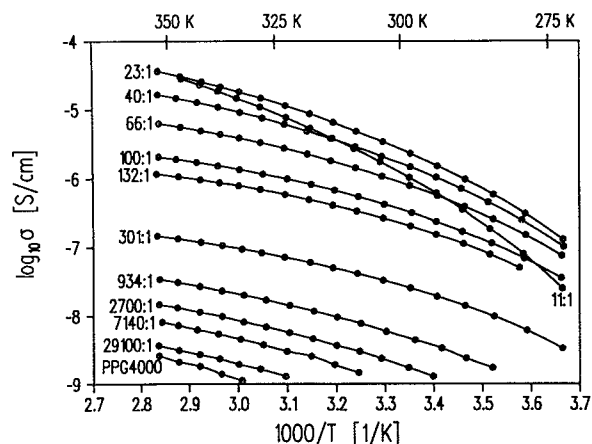


FIG. 1. The ionic conductivity plotted vs the reciprocal temperature for the PPG 4000–LiCF₃SO₃ complex for a range of concentrations given as the ratio of ether oxygen to lithium (O:Li).

using a Platel II thermocouple and the measurements were performed in a nitrogen atmosphere.

The DSC measurements were performed using a Mettler DSC-30 apparatus. The heating rate was 5 K/min and T_g was determined from the point of inflection on the DSC curve. These measurements were also performed in a dry nitrogen atmosphere.

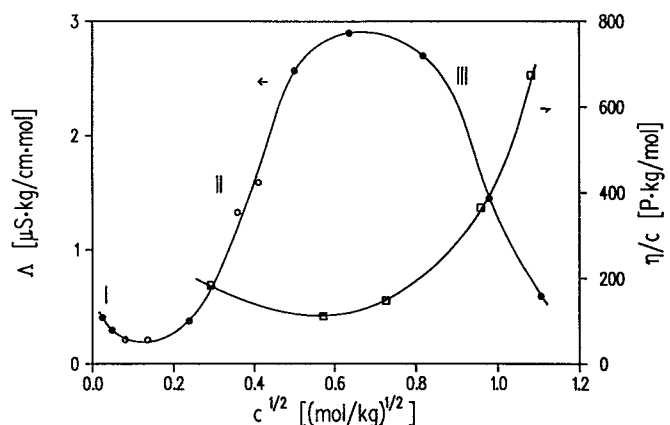
III. RESULTS

Figure 1 shows a plot of $\log_{10} \sigma$ vs reciprocal temperature for LiCF₃SO₃ dissolved in PPG 4000 for a wide range of salt concentrations. Values of σ for pure PPG 4000 are also included for higher temperatures. Notice that σ reaches a maximum for O:M \approx 20:1; this maximum is a function of temperature and salt concentration. This behavior has been reported by a number of authors for various salts in polyethers.^{2,14,24} Gray²⁴ studied a range of concentrations similar to ours for LiClO₄ in an amorphous solid ethylene oxide polyether (weight-averaged molecular weight $\bar{M}_w = 10^5$) and a low molecular weight polymer tetraethylene glycol dimethyl ether.

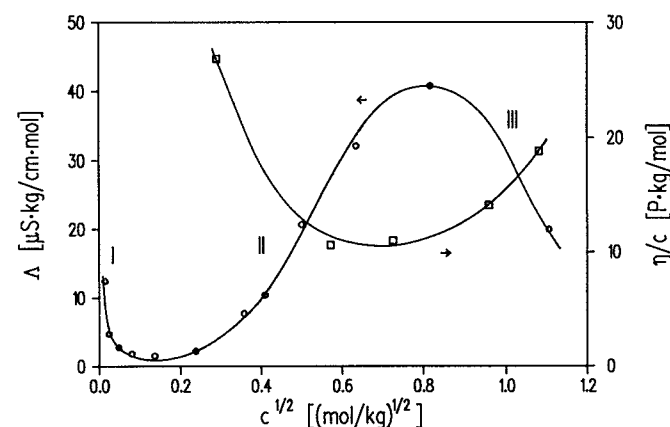
In order to see the concentration dependence for σ , it has been customary to plot the molar conductivity vs the square root of the molar concentration. For the most part, we use a concentration c of salt in moles salt per kilogram of salt plus PPG, which if multiplied by the density [$\rho = \rho(c, T)$] of the solution at that concentration and at a particular temperature, gives the molar concentration. This is seen in Fig. 2 for PPG 4000–LiCF₃SO₃ complexes where the variation of $\Lambda (= \sigma/c)$ with $c^{1/2}$ is shown for 295 K [Fig. 2(a)] and 343 K [Fig. 2(b)]. Λ_m for a charge carrier of type m is proportional to the product of the mobility μ_m and the fraction of mobile charge carriers α_m since

$$\sigma = \sum \alpha_m c_m q_m \mu_m \quad (11)$$

for charge carriers of concentration c_m and charge q_m . Three regions are identified in Fig. 2, region I at low salt concentra-



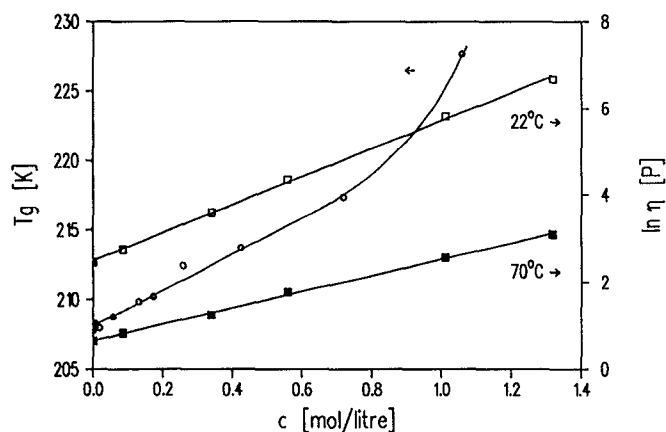
(a)



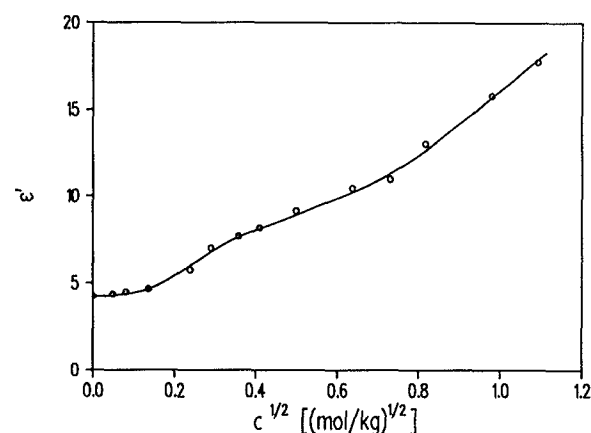
(b)

FIG. 2. (a) The molar ionic conductivity and the shear viscosity per unit of concentration plotted vs the square root of the concentration for the PPG 4000–LiCF₃SO₃ complex at 295 K. (b) The molar ionic conductivity and the shear viscosity per unit of concentration plotted vs the square root of the concentration for the PPG 4000–LiCF₃SO₃ complex at 343 K. The regions I, II, and III are discussed in the text. The curves are drawn as guides to the eye.

tions, where Λ decreases with increase in c , region II where Λ increases with increasing c to a maximum, and region III where Λ again decreases. The variation of η/c with concentration is also shown in Fig. 2. The fall in Λ is related to the rapid increase in viscosity {and T_g [Fig. 3(a)]} at higher concentrations. In Fig. 3(a) in which molar concentrations are used (see Table I), we also show that $\ln \eta$ is linear with c at both 295 and 343 K over the concentration range of the viscosity measurements. Thus $\eta = \eta_0 \exp(bc')$, where η_0 is the shear viscosity of the pure PPG, b is a function of temperature, and c' is the molar concentration. Comparing this equation with Eq. (2), we see that at a particular temperature, the molar concentration $c' \propto 1/\nu_f$; this is consistent with increases in cross linking and density²⁵ with increases in concentration. As can be seen from Fig. 3(a), $b(T)$ decreases with increase in temperature [$b(295 \text{ K}) = 3.23$ and $b(343 \text{ K}) = 1.93$]. If we use c [mol/kg (total)], we still get a straight line for $\ln \eta$ vs c [$\eta = \eta_0 \exp(bpc)$], where $bp(295 \text{ K}) = 3.63$ and $bp(343 \text{ K}) = 2.10$. Values of the shear vis-



(a)



(b)

FIG. 3. (a) The shear viscosity at 22 °C (295 K) and 70 °C (343 K) plotted vs concentration. Straight lines connect the points. A plot of the glass transition temperature vs concentration is also shown for information. (b) The permittivity plotted vs the square root of the concentration. The curve is drawn as a guide to the eye.

cosity of pure PPG, η_0 , are listed in Table II and follow a VTF form. For information, we have also plotted the permittivity [$\epsilon'(0)$] of these polyether-salt complexes as a function of $c^{1/2}$ at 293 K in Fig. 3(b).

Figure 4 is a plot of Λ vs $c^{1/2}$ for both PPG 4000-

TABLE II. Viscosity for pure PPG 4000.

T (°C)	η (P)
10.0	23.0
13.5	20.0
16.4	15.9
19.5	13.3
23.5	10.7
31.0	7.4
32.2	5.4
48.2	3.6
54.0	2.9
60.2	2.4
65.5	2.1
74.3	1.8
80.0	1.5

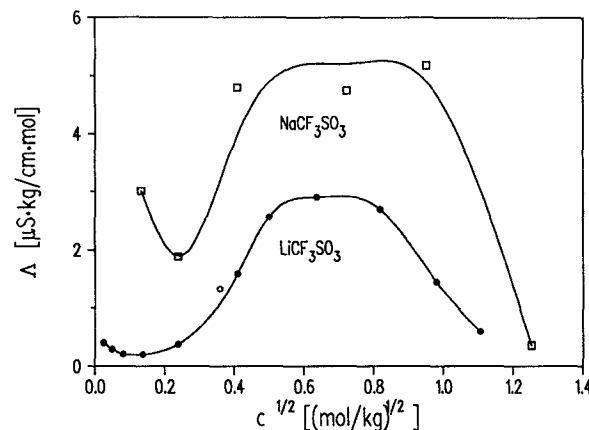


FIG. 4. The molar ionic conductivity plotted vs the square root of the concentration for PPG 4000-MCF₃SO₃ (M = Li, Na) complexes at 300 K. The curves are drawn as guides to the eye.

LiCF₃SO₃ and PPG 4000-NaCF₃SO₃ at 300 K where the polyether-sodium salt has the higher conductivity. We also observed this for poly(ethylene oxide) modified poly(dimethylsiloxane) in which the conductivity increased as the cation in the triflate went from Li to Na to K²⁶ as also observed by Watanabe *et al.* for MSCN (M = Li, Na, K) in a polypropylene oxide (PPO) network consisting of PPO triol ($\bar{M}_w = 3000$) cross linked by toluene-2,4-diisocyanate.²⁷ Blonski *et al.*²⁸ show that at higher temperatures (> 310 K), LiCF₃SO₃ in linear poly(alkoxy)phosphazene (MEEP) is a better ionic conductor than NaCF₃SO₃ in MEEP. Our results²⁶ do not agree with this finding for temperatures < 350 K.

In order to see the effect of molecular weight, we have plotted Λ vs $c^{1/2}$ in Fig. 5 for PPG 425-LiCF₃SO₃ and PPG 4000-LiCF₃SO₃ at 303 K. McLin and Angell give σ data for PPG 425-NaCF₃SO₃ and PPG 4000-NaCF₃SO₃ at one concentration (O:M = 16:1) as a function of temperature.²⁹ They also give results for η for these two complexes.

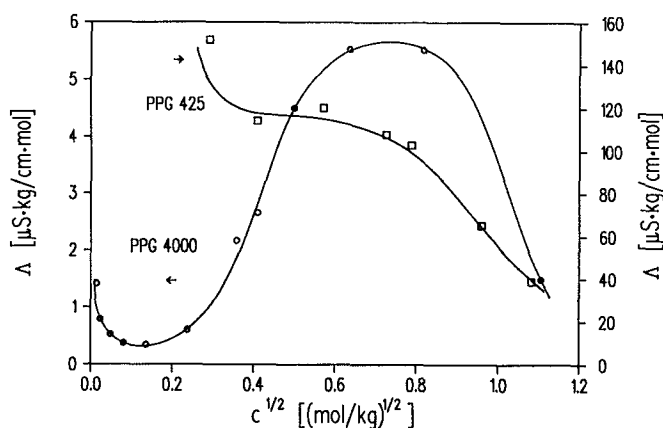


FIG. 5. The molar ionic conductivity plotted vs the square root of the concentration for PPG 425 and PPG 4000 complexed with LiCF₃SO₃ at 303 K. The curves are drawn as guides to the eye.

TABLE III. VTF parameters and temperatures of the inflection point for PPG 4000 + LiCF₃SO₃.

O:M	<i>c</i> (mol/kg)	Conductivity				Viscosity		
		<i>A</i> _σ (μs K ^{1/2} /cm)	<i>T</i> ₀ (K)	<i>T</i> _{in} (K)	<i>E</i> _σ / <i>k</i> _B (K)	<i>A</i> _η (K ^{1/2} /P)	<i>T</i> ₀ (K)	<i>B</i> (K)
∞	0	373	202	514
7140	0.002 34	11.5	199	466	661
2700	0.006 44	13.5	205	439	572
934	0.018 4	24.5	204	425	539
301	0.056 7	45.4	216	377	381
200	0.085 1	294	209	482
132	0.128	307	221	368	345
100	0.168	714	219	381	384
66.1	0.250	3 900	213	413	482
50	0.327	1150	189	828
39.8	0.405	18 400	211	446	573
30	0.527	954	193	856
23.0	0.669	95 500	205	497	724
16	0.923	2000	190	1110
15.2	0.960
12	1.174	6840	177	1500
11.4	1.223	476 000	202	590	982

IV. DISCUSSION

We have fitted the VTF relation (1) to all measured conductivity and viscosity data. In Table III and Fig. 6, the results of least-squares fits are shown for the PPG 4000–LiCF₃SO₃. In Fig. 6(a) we have plotted A_σ/c vs $c^{1/2}$ in order to indicate the dependence of the prefactor A_σ in Eq. (1) on the fraction of charge carriers since the charge carrier density $n = \Sigma \alpha_m c_m$. The variation indicated in Fig. 6(a) shows a minimum similar in form to that seen in Figs. 2(a) and 2(b). Figures 6(b) and 6(c) show the interaction between T_0 and E_σ/k_B . We should emphasize that the variation demonstrated in Fig. 6 results from the best least-squares fit to the data. T_0 vs $c^{1/2}$ should mirror the behavior for T_g as a function of concentration. There is an obvious discrepancy. In the first place, T_0 is not 35–50 K below T_g ; for some fits at low concentrations (O:M > 100:1), T_0 is even larger than T_g . Fitting a power law, $\sigma \sim (T - T_0)^{-x}$, we were able to obtain fits which were almost comparable to the VTF fits and for which x varied between 2 and 4. Values of T_0 had the same trends as for the VTF fits. This is at variance with recent evidence from a study of an ethylene oxide (EO)/propylene oxide (PO) ($M_w = 2900$) block copolymer complexed with LiI by Xue and Angell³⁰ in which, for an O:Li concentration range from 80 to 8, T_0 obtained from a VTF fit is 35–40 K below measured values of T_g . These authors used Eq. (1) without the $T^{-1/2}$ dependence in the prefactor. Fitting our data in this way produced slightly poorer fits, but gave essentially the same results as shown in Fig. 6. For $c^{1/2}$ above about 0.4 (mol/kg)^{1/2} (i.e., above the minimum in A_σ/c), the behavior of E_σ/k_B with concentration [Fig. 6(c)] is as would be expected, following the viscosity. Also shown in Fig. 6(a) is a plot of the prefactor A_η for the viscosity data for the PPG 4000–LiCF₃SO₃ system fitted to Eq. (2) with $B = T^{1/2}/A_\eta$, demonstrating even more dramatically the effect of viscosity as the salt concentration increases.

In order to understand the unexpectedly high values of T_0 at low concentrations, we examine the VTF equation in more detail. The least-squares fit of the conductivity data to the VTF equation is made assuming that n is independent of temperature. However, the number of free ions in region II is decreasing with increasing temperature and increasing with increasing concentration.^{31–33} The parameter A_σ in the VTF equation should be temperature as well as concentration dependent. The VTF equation (σ vs T) has an “S” shape with an inflection point at some temperature T_{in} . Since α is decreasing at higher temperatures, σ will not increase as much as it would if α was constant with temperature. The S shape of the VTF equation makes it possible to obtain a reasonable fit in these cases also by adjusting T_{in} (and thus T_0). In Table III, we give values T_{in} found from Eq. (1) for $d^2\sigma/dT^2 = 0$ for PPG 4000–LiCF₃SO₃ for the values of A_σ , T_0 , and E_σ/k_B obtained from VTF fits to the conductivity data. It can be seen that the value of T_{in} changes with concentration decreasing and then increasing; this behavior is opposite to that found for T_0 which increases and then decreases as the concentration increases. Thus we conclude that the strong temperature dependence of α in the region of the maximum in T_0 (minimum in T_{in}) is responsible for the unusual behavior observed for T_0 (and thus E_σ/k_B) in this region (see Fig. 6).

It has been suggested earlier that a modification of the VTF equation should include the possibility of a temperature-dependent n , but it was then assumed that α ($= \Sigma \alpha_m$) should increase with temperature.^{34,35} A modification of the VTF equation is suggested here [Eq. (12)] in which α decreases with an increase in temperature³¹

$$\sigma = A'' T^{-1/2} [1 - A' \exp(-C/k_B T)] \times \exp[-E_\sigma/k_B (T - T_0)]. \quad (12)$$

In Eq. (12), $[1 - A' \exp(-C/k_B T)]$ is proportional to the number of free ions. The parameter C ($= C'k_B/T^*$) is a

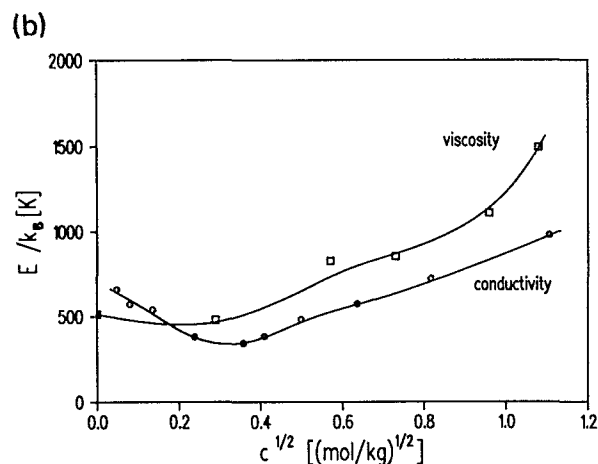
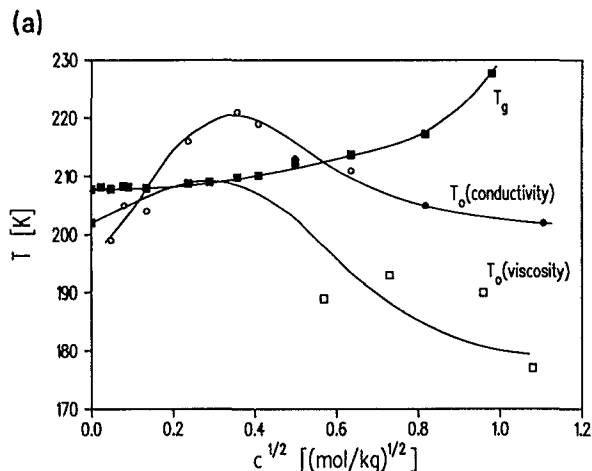
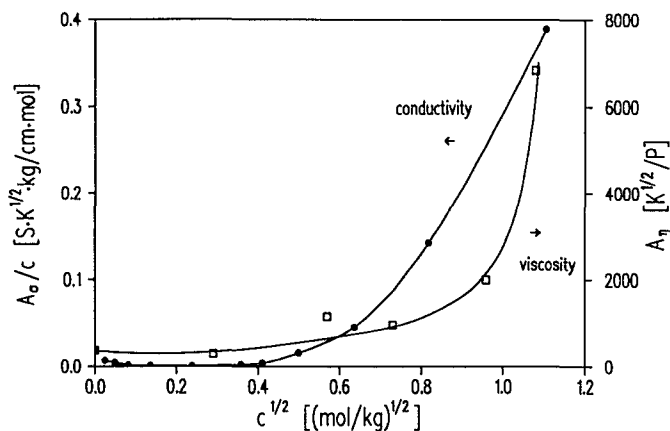


FIG. 6. (a) The VTF prefactor A_0 [Eq. (1)] per unit of concentration and the VTF prefactor A_η [through $B = T^{1/2}/A_\eta$ in Eq. (2)] plotted vs the square root of the concentration. (b) The VTF parameter T_0 [Eq. (1)] and the VTF parameter T_0 [through v_η in Eq. (2)] plotted vs the square root of the concentration. The variation of the glass transition temperature (T_g) is also shown. (c) The VTF parameters E/k_B [E_σ/k_B in Eq. (1) and $v_0/\beta v_m$ in Eq. (2)] plotted vs the square root of the concentration. The curves are drawn as guides to the eye.

function of molecular weight through the dimensionless reducing parameter T^* which increases as the molecular weight increases.³¹ This description of the behavior of the number of free ions as a function of temperature and PPG

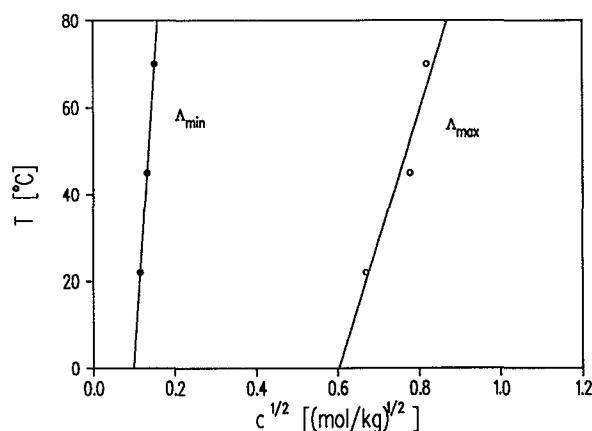


FIG. 7. The temperature at which the minimum (Λ_{\min}) and maximum (Λ_{\max}) of the molar ionic conductivity occur plotted vs the square root of the concentration.

molecular weight has been observed for the PPG 4000– NaCF_3SO_3 complex O:Na = 16:1.³¹ Using the fitting parameters obtained previously,³¹ viz. $A' = 4.051$, $C' = 1014$, and $T^* = 1.69$, with the PPG 4000– LiCF_3SO_3 (O:Li = 16:1) conductivity data, a better fit was obtained giving $T_0 = 175$ $A'' = 135.4$ and $E_\sigma/k_B = 1629$. The value of T_0 is now within the expected range of 35–50 K below T_g .

In a recent Raman study for a similar salt system,³² it has been shown that the minimum in Λ corresponds to a minimum in the fraction of free ions α when Λ or α is plotted vs $c^{1/2}$. The position of the maximum and the minimum in the Λ plot (Fig. 2) is also dependent on temperature; both seem to move to higher concentrations when the temperature increases. In Fig. 7, the temperature T at which the maximum (Λ_{\max}) and the minimum (Λ_{\min}) of the molar conductivity occurs is shown plotted against $c^{1/2}$. Since the line in Fig. 7 (Λ_{\min}) separating regions I and II represents the maximum concentration of ion pairs, one might suggest that if the fraction of free ions has a constant high value at the line, the fraction of free ions increases with increasing temperature in region I.

The ionic conductivity as a function of the salt concentration c is illustrated as a plot of Λ vs $c^{1/2}$ (see Figs. 2 and 4). $\Lambda = \sigma/c \propto \Sigma \alpha_m \mu_m$ if we assume equal concentrations and charges for the carriers [see Eq. (11)]. Thus the curve in Fig. 2 describes the product $\Sigma \alpha_m \mu_m$ vs $c^{1/2}$. The mobility μ_m is controlled by the flexibility of the polymer chain. If the temperature is constant, it is not expected that the mobility will change considerably in region I since the glass temperature T_g increases only very slightly with increasing concentration according to our DSC measurements [see Figs. 3(a) and 6(b)]. In this regard, it is instructive to plot $\eta(c, T)$ at $T = 295$ K vs $T_g(c)$ (see Fig. 8 in which two distinct linear regions are evident in the plot). Since transient cross linking by free cations occurs in the sample, this will lead to a stiffening of the polymer; an increase in T_g and a decrease in μ_m will occur. The break in the $\eta(c, T)$ vs $T_g(c)$ plot occurs at a concentration just below the Λ_{\max} region at a viscosity of

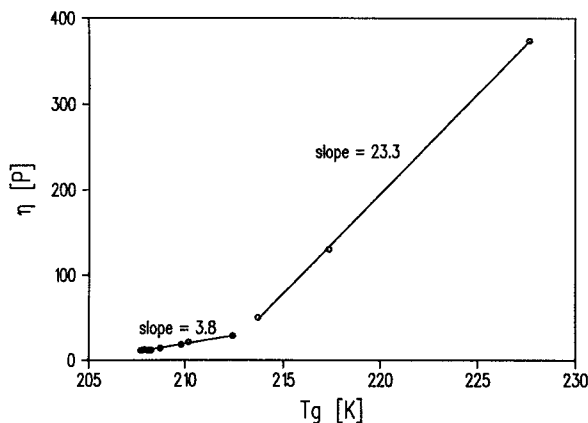
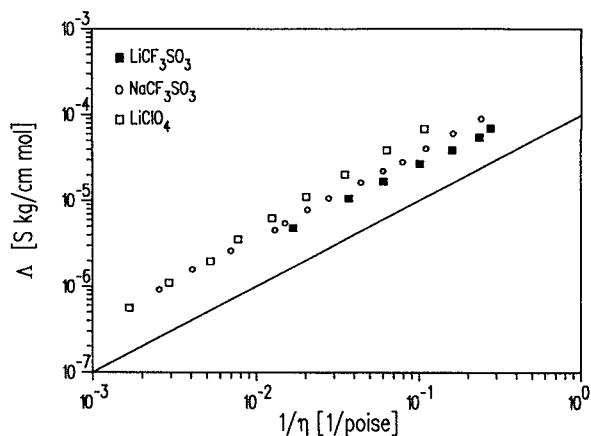


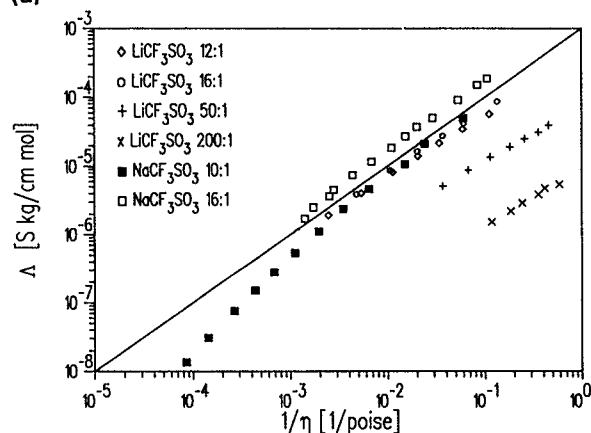
FIG. 8. The viscosity at 295 K plotted vs the glass transition temperature.

about 50 poise, but if the mobility is dependent on the number of transient cross links, then μ_m is a function of the number density of free ions n ($= \Sigma \alpha_m c_m$). Since α in region I is decreasing when c ($= \Sigma c_m$) is increasing, it is hard to predict whether n will increase or decrease. However, if n decreases, the " μ_m " will increase. We have performed a careful study of T_g in the low concentration range to see if there is any T_g dependence due to the variation of α , but the changes in T_g are very small and no firm conclusions can be made about the extent of the effect of cross linking on T_g . We will thus assume that the mobility decreases only slightly in region I and for the low concentration range in region II. In analogy with the theory for liquid solutions of ionic salts,³⁶ the drop in Λ in region I is also due to an increasing fraction of ion pairs, i.e., a decrease in α . In region II, the increase in Λ is due to an increasing fraction of charge carriers, if the mobility is not increased substantially. For polymer electrolytes, it has been suggested that either redissociation takes place, i.e., α increases with increase in c , or that an increase in the number of triple ions contributes to an increase in the conductivity.^{2,37} In region III, the pronounced increase in the viscosity and the appearance of larger aggregates are proposed as mechanisms to depress the ionic conductivity and thus Λ . As pointed out above, it has been shown that the Λ minimum corresponds to a minimum in α .³² It was also shown that redissociation is a major cause for the increase of Λ in region II³² and this is confirmed by some recent Raman measurements on the PPG-LiCF₃SO₃ system.³³

To examine the Walden rule, we have plotted Λ vs $1/\eta$ on a log₁₀-log₁₀ scale in Fig. 9. In Fig. 9(a), the concentration 30:1 is shown for LiCF₃SO₃, NaCF₃SO₃, and LiClO₄ in PPG 4000. Figure 9(b) contains Walden plots for PPG 4000-LiCF₃SO₃ (O:M = 12, 16, 50, and 200:1) and PPG 4000-NaCF₃SO₃ (O:M = 10 and 16:1). Also shown in Fig. 9 is a line of unity slope for comparison purposes. Values of the product $\Lambda\eta$ for selected temperatures are given in Table IV. Strictly speaking, the product $\Lambda\eta$ is not the Walden product since we have not taken Λ at infinite dilution. The product $\Lambda\eta$ is not constant, independent of temperature; it varies with temperature, salt concentration, and variety of salt. (Table IV also includes values for PPG 4000-LiClO₄.)



(a)



(b)

FIG. 9. (a) The "Walden" plot of the molar ionic conductivity vs the reciprocal of the shear viscosity for PPG 4000 with LiCF₃SO₃, NaCF₃SO₃, and LiClO₄ (O:M = 30:1). The straight line has a slope of one. (b) The Walden plot of the molar ionic conductivity vs the reciprocal of the shear viscosity for various concentrations of MCF₃SO₃ (M = Li, Na) in PPG 4000. The straight line has a slope of one.

TABLE IV. $\Lambda\eta$ for LiCF₃SO₃, NaCF₃SO₃, and LiClO₄ (A) at 300; (B) at 325; and (C) at 350 K.

	O:M	$\Lambda\eta$ [s kg P/cm mol ($\times 10^{-3}$)]		
		LiCF ₃ SO ₃	NaCF ₃ SO ₃	LiClO ₄
(A)	10		0.415	1.501
	12	0.792		
	16	0.810	1.699	
	30	0.284	0.374	0.508
	50	0.136		
(B)	200	0.014		
	10		0.719	1.696
	12	0.701		
	16	0.768	1.713	
	30	0.272	0.362	0.614
(C)	50	0.113		
	200	0.012		
	10		0.842	1.939
	12	0.580		
	16	0.666	1.762	
	30	0.230	0.358	0.564
	50	0.088		
	200	0.010		

Assuming that $\eta \propto 1/\mu$ [cf. Eq. (4)], the product $\Lambda\eta$ in region II may be described in a simple way using Eq. (11) assuming only one kind of charge carrier

$$\Lambda\eta \propto \sigma/c\mu = \alpha q.$$

Thus, $\Lambda\eta$ is proportional to the fraction of free ions α . For region II ($O:M > 16:1$), $\Lambda\eta$ increases with an increase in concentration and decreases with increasing temperature (see Table IV). This agrees with the reported trends for α ,^{32,33} i.e., α increases with an increase in concentration and decreases with an increase in temperature. One might also expect this temperature behavior from Eq. (6) [combined with Eq. (3)] if above T_g the cross-linked polyether can be considered to be an elastomer in which c_s varies inversely as temperature.³⁸ The concentration dependence of $\Lambda\eta$ is more difficult to see from Eq. (6) since, for the dynamic bond percolation model, p is a constant and α is independent of the concentration. Thus $\Lambda\eta$ should decrease with an increase in temperature due to c_s . The mechanical shear velocity has a much higher temperature coefficient ($\approx -10 \text{ ms}^{-1} \text{ K}^{-1}$) than the mechanical longitudinal velocity ($\approx -0.2 \text{ ms}^{-1} \text{ K}^{-1}$). Thus if it is the shear velocity that is important in Eq. (6), then a larger decrease in $\Lambda\eta$ with increase in temperature would be observed due to c_s .

In Table IV [and Fig. 9(a)], the larger values of $\Lambda\eta$ for PPG 4000- NaCF_3SO_3 than for PPG 4000- LiCF_3SO_3 (see $O:M = 30:1$ and $16:1$) are because the ion conductivity in the former is higher; in fact, at 300 K, for $O:M = 16:1$, α for the sodium complex is 0.44 and for the lithium complex is 0.31. The viscosity for the sodium complex is only slightly lower than for the lithium complex^{14,25}; Na^+ is less a structure maker than is Li^+ . For the PPG 4000- LiClO_4 complex, which has the highest magnitudes for $\Lambda\eta$, the viscosity is higher and the conductivity only slightly lower than for the PPG 4000- LiCF_3SO_3 complex. However, as can be seen in Fig. 9(a) at high viscosities (lower left-hand part of the graph), the points come together indicating that the viscosity of the PPG-salt complex is independent of the salt. Also, at $O:M = 30:1$, the Walden plots are approximately linear with slopes close to unity. In Fig. 9(b), we see evidence of the conductivity maximum reflected in the Walden plots especially for PPG 4000- LiCF_3SO_3 . The higher conductivity for PPG 4000- NaCF_3SO_3 is also shown.

Incorporating Eq. (8) into Eq. (3), we have attempted to fit our PPG 4000- LiCF_3SO_3 conductivity data at low concentrations (as advised by Ratner³⁹) to the dynamic percolation model of Ratner *et al.*,^{3,10} but were unable to identify a concentration dependent term. However, if we assume p varies as c^{-1} in Eq. (8), as one might expect if ion-ion effects were incorporated, and combine the result with Eq. (3), we obtain a fit for this conductivity data with a value of 0.75 for the exponent for low concentrations and up to 0.17 mol/kg. There would be a similar result if we used $p \sim c^{-1}$ in Eq. (10) combined with Eq. (3).

If we speculate that clusters are formed as mentioned in the Introduction, Eq. (9) might be used to estimate the concentration dependence of the conductivity over the whole range. In Fig. 10, we show a fit to the data of Fig. 2(a) using Eq. (9) divided by the concentration and η/η_0 . We used

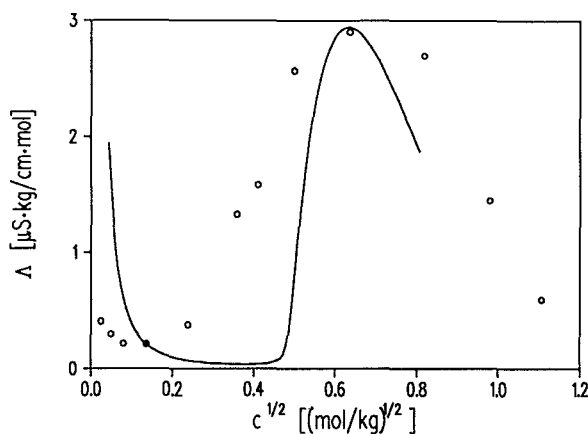


FIG. 10. The data of Fig. 2(a) (O) (molar ionic conductivity vs the square root of the concentration) fitted to Eq. (9) divided by the concentration and bulk shear viscosity (solid line).

values of $\sigma_1 (= 1.2 \times 10^{-6} \text{ S/cm})$ and $\sigma_2 (= 3.8 \times 10^{-9} \text{ S/cm})$ taken, respectively, from the concentration (0.67 mol/kg) at which the maximum conductivity occurs and from the concentration (0.02 mol/kg) at which the minimum molar conductivity occurs. For low concentrations, the local or microscopic viscosity should remain low and not change significantly until a concentration $\sim 0.15 \text{ mol/kg}$. This is not reflected in the bulk shear viscosity and so the abrupt behavior of the fitted curve in Fig. 10 around values of $c^{1/2} \sim 0.4 \text{ (mol/kg)}^{1/2}$ would be softened. Although the agreement between the fitted values and the experimental results is only fair, we conclude that a "stirred" model of regions of clusters of solvent separated, charged ions and charged aggregates interspersed with regions of very low ionic conductivity might be applied for these systems.

In this study, we have compared the conductivities using polymers with two different molecular weights. If we compare the viscosity η of the pure polymer multiplied by the molal conductivity Λ for samples with 0.1 mol% LiCF_3SO_3 (0.018 mol/kg) at 20 °C, we get $\Lambda\eta$ values of 2.38×10^{-5} and $1.57 \times 10^{-5} \text{ s kg P/mol cm}$, respectively, for PPG 425 and PPG 4000. The high ionic conductivity obtained for complexes with PPG 425 is thus due mainly to the difference in viscosity of the polymers, but it can be noted that $\Lambda\eta$ for PPG 425 is one and a half times larger than that for PPG 4000. According to Raman scattering measurements, the number of free anions is larger in complexes with PPG 400 than with PPG 4000 by a factor of about 1.7.³¹ This confirms that there are more free charge carriers in the lower molecular weight polymer.

IV. CONCLUSIONS

Conductivity results have been obtained for PPG- MCF_3SO_3 ($M = \text{Li, Na}$) complexes over a wide range of concentrations. Fitting the empirical VTF equation to our data results in a variation of the prefactor A_0 with concentration as would be expected, but the variation of the fitting parameter T_0 with concentration does not follow the vari-

ation of T_g with concentration. We conclude that this is due to the temperature dependence of the number of charge carriers and therefore of A_σ . T_0 and E_σ/k_B are interdependent parameters.

Although there is an approximate inverse relationship between conductivity and viscosity as would be expected, the Walden rule product $\Lambda\eta$ is not constant independent of temperature or concentration in our solvent PPG. In region II (O:M > 16:1), $\Lambda\eta$ increases with increasing concentration and decreases with temperature.

A Walden type relationship proposed by Ratner and Nitzan³ comes close to explaining the $\Lambda\eta$ behavior if one assumes that the probability of path availability p is proportional to concentration. However, under the same assumption, the dynamic bond percolation model of these authors together with Druger and Granek^{3,10,11} does not fit our conductivity data for low concentrations. More understanding is required concerning the interpretation of p , especially when ion-ion interactions are present. A model consisting of clusters of charged species separated by regions of very low ionic conductivity and continually being stirred with some renewal time τ_R ($\alpha\eta$) may describe the conductivity over a large concentration range; two suggestions are made, one of which gives an exponent (0.75) in agreement with random superconducting networks.

We suggest that the three regions which can be identified in the graph of molar conductivity ($\Lambda = \sigma/c$) vs the square root of the concentration can be explained in terms of first an initial drop to a minimum due to an increase in the contact ion pair concentration with a slight decrease in μ , second an increase in the fraction of charged species, mainly free ions, and third a decrease due to rapidly increasing local viscosity and formation of larger aggregates.

ACKNOWLEDGMENTS

This work was carried out with the support of the Swedish Natural Sciences Research Council and Natural Sciences and Engineering Research Council of Canada. The authors are grateful to S. D. Druger for his comments on the manuscript, to S. H. Chung, C. G. Gray, and B. G. Nickel for helpful discussions, and to Y. Fu for some of his unpublished viscosity measurements.

¹ M. B. Armand, J. M. Chabagno, and M. J. Duclot, in *Fast Ion Transport in Solids*, edited by P. Vashita, J. N. Mundy, and G. K. Shenoy (Elsevier-North Holland, New York, 1979), p. 131; J. M. Chabagno, thesis, Institut National Polytechnique, Grenoble, 1980; M. B. Armand, *Annu. Rev. Mater. Sci.* **16**, 245 (1986).

- ² G. G. Cameron and M. D. Ingram, in *Polymer Electrolyte Reviews 2*, edited by J. R. MacCallum and C. A. Vincent (Elsevier Applied Science, London, 1989), p. 157.
- ³ M. A. Ratner, in *Polymer Electrolyte Reviews 1*, edited by J. R. MacCallum and C. A. Vincent (Elsevier Applied Science, London, 1987), p. 173; M. A. Ratner and D. F. Shriver, *Chem. Rev.* **88**, 109 (1988); M. A. Ratner and A. Nitzan, *Faraday Discuss. Chem. Soc.* **88**, 19 (1989).
- ⁴ B. L. Papke, M. A. Ratner, and D. F. Shriver, *J. Electrochem. Soc.* **129**, 1694 (1982).
- ⁵ A. K. Doolittle, *J. Appl. Phys.* **22**, 1471 (1951).
- ⁶ R. Kubo, *J. Phys. Soc. Jpn.* **12**, 570 (1957).
- ⁷ Y. Gefen and I. Goldhirsch (preprint, 1987); see reference in S. Havlin and D. Ben-Avraham, *Adv. Phys.* **36**, 695 (1987).
- ⁸ J. Frenkel, *Kinetic Theory of Liquids* (Dover, New York, 1955), p. 42.
- ⁹ P. Walden, *Salts, Acids, and Bases: Electrolytes: Stereochemistry* (McGraw-Hill, New York, 1929), p. 283; *Z. Phys. Chem.* **55**, 249 (1906).
- ¹⁰ S. D. Druger, A. Nitzan, and M. A. Ratner, *J. Chem. Phys.* **79**, 3133 (1983).
- ¹¹ R. Granek and A. Nitzan, *J. Chem. Phys.* **90**, 3784 (1989).
- ¹² A. K. Harrison and R. Zwanzig, *Phys. Rev. A* **32**, 1072 (1985).
- ¹³ A. L. R. Bug and Y. Gefen, *Phys. Rev. A* **35**, 1301 (1987).
- ¹⁴ Y. Fu, K. Pathmanathan, and J. R. Stevens, *J. Chem. Phys.* **94**, 6323 (1991).
- ¹⁵ A. Killis, J. F. LeNest, H. Cheradame, and A. Gandini, *Macromol. Chem.* **183**, 2835 (1982).
- ¹⁶ M. Watanabe and N. Ogata, in *Polymer Electrolyte Reviews 1*, edited by J. R. MacCallum and C. A. Vincent (Elsevier Applied Science, London, 1987), p. 39; *Brit. Polymer J.* **20**, 181 (1988).
- ¹⁷ S. Havlin and D. Ben-Avraham, *Adv. Phys.* **36**, 695 (1987).
- ¹⁸ D. G. Ast, *Phys. Rev. Lett.* **33**, 1042 (1974).
- ¹⁹ S. Kirkpatrick, *Rev. Mod. Phys.* **45**, 574 (1973).
- ²⁰ R. Landauer, *J. Appl. Phys.* **23**, 779 (1952).
- ²¹ A. Bunde, W. Dieterich, and E. Roman, *Phys. Rev. Lett.* **55**, 5 (1985).
- ²² H. E. Roman, A. Bunde, and W. Dieterich, *Phys. Rev. B* **34**, 3439 (1986).
- ²³ D. Stauffer, *Introduction to Percolation Theory* (Taylor and Francis, London, 1985).
- ²⁴ F. M. Gray, *Solid State Ion.* **40** and **41**, 637 (1990).
- ²⁵ W. Wixwat, Y. Fu, and J. R. Stevens, *Polymer* **32**, 1181 (1991).
- ²⁶ I. Albinsson, P. Jacobsson, B.-E. Mellander, and J. R. Stevens, *Polymer* **32**, 2712 (1991).
- ²⁷ M. Watanabe, K. Nagaoka, M. Kanba, and I. Shinohara, *Polymer J.* **14**, 877 (1982).
- ²⁸ P. M. Blonsky, D. F. Shriver, P. Austin, and H. R. Allcock, *Solid State Ion.* **18** and **19**, 258 (1986).
- ²⁹ M. McLin and C. A. Angell, *J. Phys. Chem.* **92**, 2083 (1988).
- ³⁰ R. Xue and C. A. Angell, *Solid State Ion.* **25**, 223 (1987).
- ³¹ S. Schantz, L. M. Torell, and J. R. Stevens, *J. Chem. Phys.* **94**, 6862 (1991).
- ³² S. Schantz, *J. Chem. Phys.* **94**, 6296 (1991).
- ³³ J. R. Stevens and P. Jacobsson, *Can. J. Chem.* (in press for Dec. 1991).
- ³⁴ H. Cheradame, in *IUPAC Macromolecules*, edited by H. Benoit and P. Rempp (Pergamon, New York, 1982), p. 351.
- ³⁵ M. Watanabe, K. Sanui, N. Ogata, T. Kobayashi, and Z. Ohtaki, *J. Appl. Phys.* **57**, 123 (1985).
- ³⁶ J. O. M. Bockris and A. K. N. Reddy, *Modern Electrochemistry* (Plenum, New York, 1970), Vol. 1.
- ³⁷ G. G. Cameron, J. L. Harvie, M. D. Ingram, and G. A. Sorrie, *Brit. Polymer J.* **20**, 199 (1988).
- ³⁸ J. R. Cunningham and D. G. Ivey, *J. Appl. Phys.* **27**, 967 (1956), see also, *The Polymer Handbook*, 3rd ed., edited by J. Brandrup and E. H. Immergut (Wiley, New York, 1989), p. V/7.
- ³⁹ M. A. Ratner, *Faraday Discuss. Chem. Soc.* **88**, 89 (1989).